Analysis of the Three-Dimensional Nanoscale Relationship of Ge Quantum Dots in a Si Matrix Using Focused Ion Beam Tomography.

Alan J. Kubis[1], Thomas E. Vandervelde[2], John C. Bean[3], Derren N. Dunn[4], Robert Hull[1]
[1]Univ. of Virginia, Dept of Materials Science and Engineering, Charlottesville, VA 22904, U.S.A; [2]Univ. of Virginia, Dept of Physics, Charlottesville, VA 22904, U.S.A; [3]Univ. of Virginia, Dept of Electrical and Computer Engineering, Charlottesville, VA 22904, U.S.A; [4]Now at IBM Microelectronics, Hopewell Junction, NY 12533, U.S.A.

ABSTRACT

It is well documented that buried layers in quantum dot (QD) superlattices influence the position of quantum dots in the subsequently grown layers through strain field interactions (e.g.[1,2, 3,4]). Using the Focused Ion Beam (FIB) tomographic technique we have reconstructed the 3D relationship of successive layers of coherent Ge QDs separated by epitaxial Si capping layers – a "QD superlattice".

Techniques such as Atomic Force Microscopy (AFM) and Scanning Tunneling Microscopy (STM) can only look at a single surface layer of QDs or, in the case of Transmission Electron Microscopy (TEM), look at a two-dimensional projection of a three-dimensional volume so that 3D relationships need to be inferred. Since the strain interactions are complex, an enhanced fundamental understanding of these self-organization mechanisms can more directly be obtained from full 3D reconstructions of these structures.

By capping with Si at 300°C we were able to grow QD superlattices with QDs tens of nanometers in height. This places them within the resolution of the FIB tomographic technique to reconstruct. Using the FIB we performed *in-situ* serial sectioning of the QD superlattice and then reconstructed the QD superlattice. The reconstruction was then analyzed to investigate the ordering of the QDs.

Results from a reconstruction of a superlattice matrix will be presented with analysis of the self-ordering of the QDs. Observations of a novel self-limiting (in height) morphology, the quantum mesa, associated with the capping technique used will also be discussed.

INTRODUCTION

Much work has been done to study the phenomenon of self-assembly in quantum dot systems (e.g.[1-8]). Multi-layered structures, known as superlattices, are seen to organize so that the Quantum Dots (QDs) on successive layers nucleate and grow above the buried QDs[5]. The self-assembly occurs such that the QDs in the later layers deviate from being centered on the lower QDs to positions that more evenly space the quantum dots. The driving force for this is believed to be due to minimization of the system strain energy driven by QD-QD interaction energies in lattice mismatched systems[6,7,8]. In the past techniques such as Transmission Electron Microscopy (TEM), Scanning Tunneling Microscopy (STM) and Atomic Force Microscopy (AFM) have been used to analyze these structures. In the case of STM and AFM only the top most layer can be observed while TEM gives a two-dimensional projection of a three-dimensional volume. In several papers models have been presented that explore this phenomenon but in all cases are based on these two-dimensional observations.

In this study the ordering of Ge QDs in a Si matrix was investigated. When grown on Si, Ge first forms a wetting layer due to its lower surface energy. As the thickness of the Ge layer increases, strain energy in the system increases due to the 4.1% lattice mismatch between Si and

Ge (Ge having the larger lattice constant). At a characteristic thickness, islanding of the Ge initiates as a stress relief mechanism[6]. This type of growth is known as Stranski-Krastanov (SK) growth[9,10]. As the islands (QDs) grow they go through a transition from initial hut clusters with {105} facets and a square base to coherent domes with predominantly {113} facets, to dislocated domes when the strain cannot be sufficiently relieved by islanding alone[11,12,13].

To gain a greater insight into these self-assembly processes, the focused ion beam was used to serial section a superlattice. The three-dimensional sample volume was them tomographically reconstructed so that the self-assembly could be investigated. To maintain the initial QD morphologies overgrowth of the QDs, the Si capping between layers of QDs was performed at a temperature significantly lower than the QD growth temperature so that the aspect ratio of the as grown QDs was retained.

EXPERIMENTAL DETAILS

Ge and Si films were grown via molecular-beam epitaxy (MBE) on (001) Si substrates using a custom built VG 90S double-chamber UHV-MBE system at the University of Virginia (UVa)[14]. Before sample growth, a modified "piranha clean" procedure was employed to clean and hydrogen-passivate the substrates[15]. The resulting hydrogen-terminated layer, along with any surface oxide, was desorbed at a temperature of 775°C. A typical sample growth used in this study constituted the deposition of a 1000Å Si buffer layer at a starting temperature of 775°C. The substrate temperature was progressively lowered to the Ge growth temperature, 750°C, during deposition of the buffer layer. This procedure allows for immediate growth of the epilayer, thereby eliminating any chance of contamination buildup. Once the Ge was deposited the sample was cooled to a "cold" Si capping layer temperature of 300°C[16]. The temperature was then increased for deposition of a "hot" Si cap at the original Ge deposition temperature. Growths were done at 100% Si or Ge. When growing the superlattice structure a 20nm cold cap was followed by an 80nm hot cap. The three growth steps were repeated 20 times for the superlattice. The base pressure in the chamber prior to growth was typically $2x10^{-10}$ Torr. The samples were then analyzed by TEM and, in the case of the superlattice, by the FIB tomographic technique.

TEM cross sectional foils (i.e electron beam approximately parallel to epitaxial interfaces) were prepared by standard 4-6 keV Ar^+ ion beam thinning techniques. TEM analysis was performed using a JEOL FX2000 TEM[17], operated at 200 kV, with a dual tilt holder. All analyses were performed using the [011] zone axis, the specific imaging conditions for each image are given in the relevant figure captions.

Focused Ion Beam (FIB) serial sectioning was performed using an FEI FIB-200[18] with a Ga ion source. The sample was milled in serial fashion by positioning the surface of interest parallel to the beam direction and removing material with the outside edge of the beam. When a flat surface was obtained the sample was rotated 90° such that the newly formed surface was normal to the primary ion beam and the resultant surface was imaged with secondary electrons. This procedure was repeated at 20nm intervals until the total volume of interest was sectioned. The images were processed using Adobe Photoshop[19] with the Fovea Pro[20] tool kit to increase contrast and, in the case of shape-based interpolation method, to find the edges of quantum dot features. MATLAB[21] was used to reconstruct the sectioned volume via a linear interpolation method. In this case the volume between the slices was filled by linearly interpolating the intensity of the equivalently positioned pixels in adjacent slices. Shape-based interpolations were calculated using computer code developed at UVa[22,23]. Here the edges of the QD features are initially found. A bilinear interpolation method uses the position of the edges in adjacent slices to

interpolate the position of the edge in the interpolated slices between them. This allows for a smoother transition between slices and reconstructs the curvature of the features between the experimental slices. These methods are more fully described elsewhere[24].

DISCUSSION

When QDs are capped at temperatures above 400°C they spread out so that their final height is only several nanometers and their aspect ratio decrease[25,26]. Since the spatial resolution of the FIB is of the order 10nm, retention of the original aspect ratio was desirable. Following a procedure described by Rastelli *et al.* the original aspect ratio could be retained for the QDs[27]. In brief, the QDs were initially capped at a low temperature, approximately 300°C, to completely cover the QDs. The temperature was then increased to the QD growth temperature and additional Si deposited until the desired spacer thickness was obtained. Figure 1 shows a Ge QD capped with 20nm of Si prior to increasing the temperature. There was no obvious spreading of the QD and the size distribution of the QDs was similar to uncapped QDs grown under the same conditions. When the temperature was raised and the remainder of the spacer layer deposited, something new was observed. In Figure 2 the QD near the center of the image has been truncated at a height near the thickness of the cold capping layer.
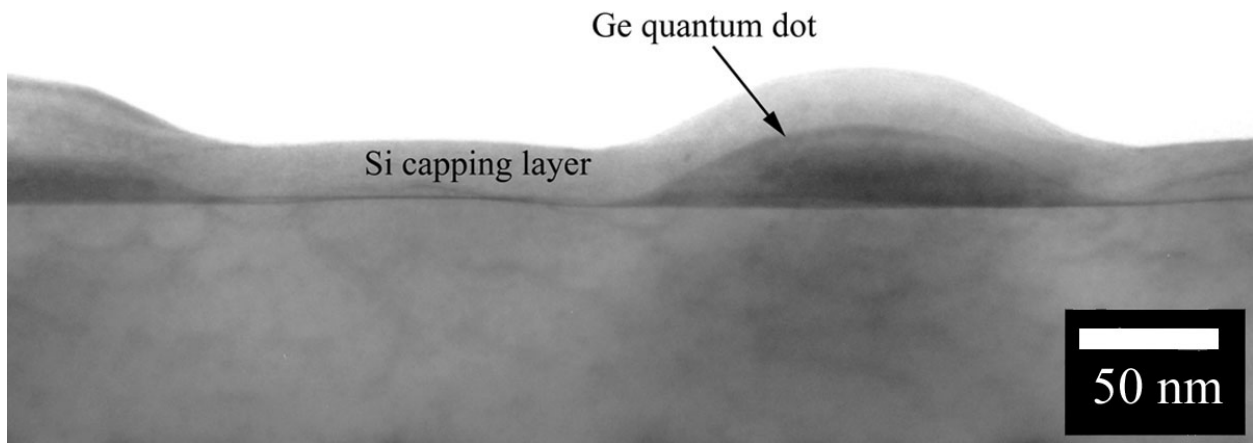

Figure 1. TEM image of Ge QD with 20nm Si cap deposited at 300°C. Image was acquired using the forward scattered beam with no strongly diffracted reflections so that the elemental ("mass-thickness") contrast could more easily be observed.
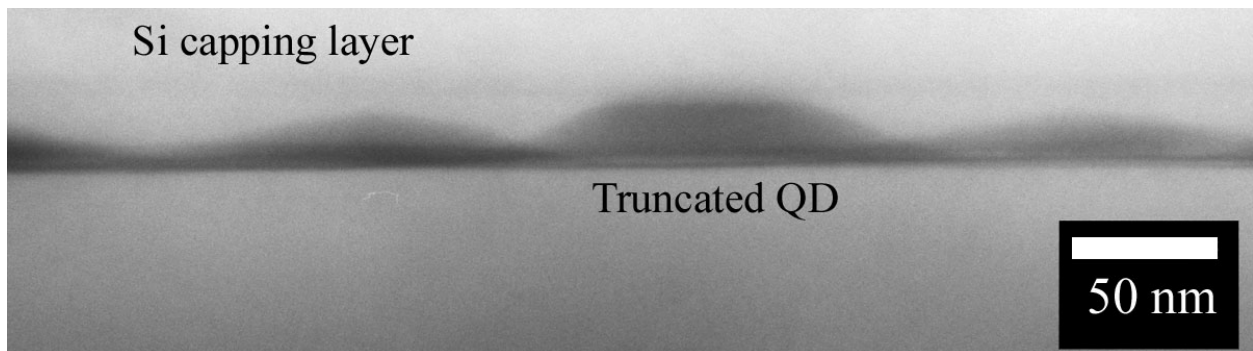

Figure 2. TEM image of truncated "Quantum Mesa". Truncation occurs at the approximate 20nm thickness of the cold cap layer. Image was acquired using the forward scattered beam with no strongly diffracted reflections so that the elemental contrast could more easily be observed.

The QDs to either side of this "Quantum Mesa" have retained their shape since their height is less than the thickness of the cold capping layer. Flattening of the Si capping layer and of the QDs being embedded has been studied by different investigators but not in the type of discontinuous growth sequence employed here[26,28].

Using this capping method a 20 layer QD superlattice was grown for FIB tomgraphic reconstruction. A TEM image of the superlattice is shown in Figure 3. Since this is a two-dimensional projection of a three-dimensional volume the precise relationship of the QD columns cannot be determined. In fact, in some cases columns overlap in projection. In other cases it is uncertain whether columns start on layers other than the first, disappear prior to the 20th layer or are not completely encased in the limited thickness (c. 100 nm) of the TEM foil. Figure 4 shows the tomographic reconstruction of the QD superlattice. This reconstruction was produced using serial slices parallel to the front face of the reconstruction and then the volume filled using the shape-based interpolation method. In the reconstruction it can be observed that QDs on upper layers grow above the QDs in the lower layers. The spatial resolution between layers in the original images was intentionally decreased in Photoshop so that the evolution of the columns is more apparent. The true relationship between the QDs and the spacing layer can more clearly be seen in Figure 3. The flat faces of the QD columns are where the initial slice intersected the column. Upon close examination of the tomographic reconstruction in Figure 4 it can be seen that all of the columns in the reconstruction do emanate from the first layer grown and in some cases are extinguished prior to the 20th layer. The termination of QD columns after several layers of growth was predicted by Tersoff *et al.* and Liu *et al.* for QD columns that were too closely spaced[3,4]. In addition when layers of QDs at successive levels are examined, such as those in Figure 5, the evolution of the self-assembly process can be directly observed. Small closely spaced QDs can easily be seen in the lower layers of the quantum dot superlattice. As some columns disappear, as seen in Figure 4, the QDs in the other columns increase in size. This clearly shows one effect of the self-assembly process.
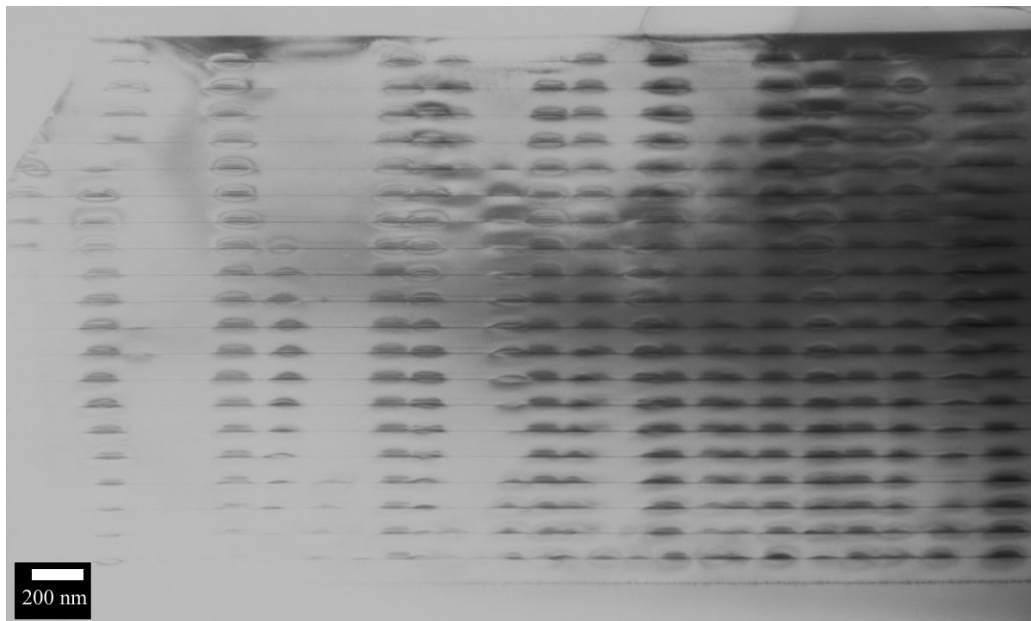
Figure 3. TEM image of Ge quantum dot superlattice in a Si matrix. Bright field image was taken using a <400> two-beam condition so that the strain contrast, due to the lattice mismatch of the embedded quantum dots with the matrix, is accentuated.
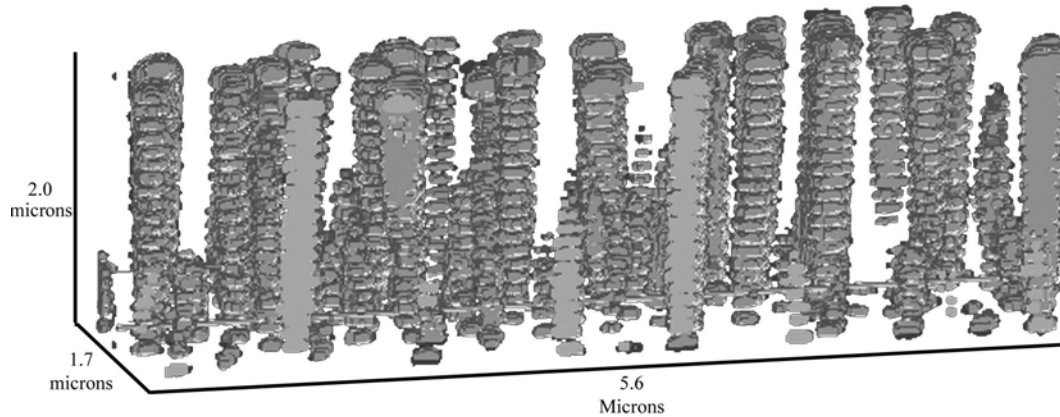
Figure 4. FIB tomographic reconstruction of the QDs in a Ge/Si quantum dot superlattice. Several quantum dot columns can be seen to terminate prior to the final 20th layer. The spatial resolution between the layers was intentionally decreased so that the evolution of the columns could more easily be observed.
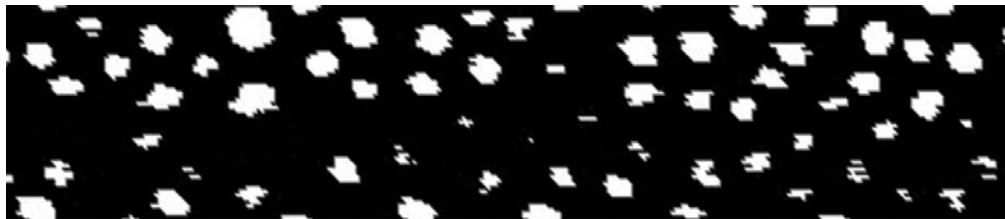
Figure 5. Reconstructed images of a lower and upper layer of the quantum dot superlattice; dimensions in both images are 1.7x5.6 microns. a). shows the lower layers of quantum dots contain small closely spaced quantum dots. b). shows the resulting lower population of larger quantum dots in the upper layers.

CONCLUSIONS

By performing tomographic reconstructions of QD superlattices the three-dimensional relationship of the QD columns can be studied directly. The actual relationship between columns and between QD layer can be directly compared to models developed to explain self-assembly and not inferred from two-dimensional techniques such as TEM and AFM.

ACKNOWLEDGMENTS

[1] G. Springholz, M. Pinczzolits, V. Holy, S. Zerlauth, I. Vavra, G. Bauer, Physica E **9**, 149-163 (2001).

[2] V. Le Thanh, V. Yam, Y. Zheng, D. Bouchier, Thin Solid Films **380**, 2-9 (2000).

[3] J. Tersoff, C. Teichert, M.G. Lagally, Phys. Rev. Lett. **76**, 1675-1678 (1996).

[4] F. Liu, S.E. Davenport, H.M. Evans, M.G. Lagally, Phys. Rev. Lett. **82**, 2528-2531 (1999).

[5] C.J. Huang, D.Z. Li, B.W. Cheng, J.Z. Yu, Q.M. Wang, Appl. Phys. Lett. **77**, 2852-2854 (2000).

[6] J. Tersoff, Phys. Rev. B **43**, 9377-9380 (1991).

[7] Madhukar, A.; T.R. Ramachandran, A. Konkar, I. Mukhametzhanov, W. Yu, P. Chen, Appl. Surf. Sci. **123/124**, 266-275 (1998).

[8] Lutz, M.A.; R.M. Feenstra, P.M. Mooney, J. Tersoff, J.O. Chu, Surf. Sci. **316**, L1075-L1080 (1994).

[9] I.N.Stranski, L.Krastanov, Akad. Wiss. Wien, Math.-Naturwiss. Kl. II b, **146**, 797 (1938).

[10] D.J. Eaglesham, M. Cerullo, Phys. Rev. Lett. **64**, 1943-1946 (1990).

[11] M. Tomitori, K. Watanabe, M. Kobayashi, O. Nishikawa, Appl. Surf. Sci. **76/77**, 322-328 (1994).

[12] F.M. Ross, R.M. Tromp, M.C. Reuter, Science **286**, 1931-1934 (1999).

[13] Y.-W. Mo, D.E. Savage, B.S. Swartzenruber, M.G. Lagally, Phys. Rev. Lett. **65**, 1020-1023 (1990).

[14] R. Hull and J.C. Bean, *Germanium Silicon: Physics and Material*, Semiconductors and Semimetals, **56**, 6 (1999).

[15] D.A. Glocker and S. I. Shah, *Handbook of Thin Film Process Technology*, Institute of Physics Publishing, E1.0:8 (1995).

[16] A. Rastelli, E. Muller, H. von Kanel, Appl. Phys. Lett. **80**, 1438-1440 (2002).

[17] JEOL LTD. Tokyo, Japan.

[18] FEI Company, Hillsboro, OR 97124.

[19] Photoshop, Version 6.0, Adobe Systems Inc., San Jose, CA 95110.

[20] Fovea Pro, Reindeer Graphics Inc., Asheville, NC 28801.

[21] MATLAB, Version 6.0, The Mathworks Inc., Natick, MA 01760.

[22] D.N. Dunn, R. Hull: Appl. Phys. Lett. **75**, 3414-3416 (1999).

[23] D.N. Dunn, G.J. Shiflet, R. Hull: Rev. Sci. Instrum., **73**, 330-334 (2002).

[24] A.J. Kubis, G.J Shiflet, D.N. Dunn, R. Hull, Met. Mater. Trans. A., In Press.

[25] J.L. Bischoff, C. Pirri, D. Dentel, L. Simon, D. Bolmont, L. Kubler, Mat. Sci. Eng. B **69/70**, 374-379 (2000).

[26] P. Sutter, M.G. Lagally, Phys. Rev. Lett. **81**, 3471-3474 (1998).

[27] A. Rastelli, E. Muller, H. von Kanel, Appl. Phys. Lett. **80**, 1438-1440 (2002).

[28] D. Dentel, J.L. Bischoff, L. Kubler, J. Werckmann, M. Romeo, J. Crystal Growth **191**, 697-710 (1998).